in: Proc. EMBC-2011, 33rd Annual Intl. Conf. of the IEEE EMBS, Boston, MA, USA, Aug. 30 - Sept. 3, 2011, pp. 2586-2589.

Topographic Imaging of the Atrial Electrical Activity During Atrial Fibrillation for the Analysis of Uniform Distributions of the Surface Electrical Potentials

Pietro Bonizzi, Olivier Meste, Vicente Zarzoso, Ronald Westra, Joël Karel, Maria S. Guillem, and Francisco Castells

Abstract— **Atrial fibrillation (AF) is a progressive arrhythmia which causes time dependent impairing of the cardiac muscle. This makes that proper therapeutic interventions depend on the degree of AF progression, i.e., on the temporal decrease of the organization of the electrical patterns observed during AF. Standard effective treatments are still lacking nowadays, and this calls for suitable noninvasive analysis of AF. In this sense, an appropriate therapy relies on the knowledge of AF characteristics, as its degree of organization. To this purpose, fast and accurate imaging of cardiac electrical activity can be helpful. Relying on the results of previous work on noninvasive assessment of the complexity of AF, we put forward a method to obtain visual maps of the topographic projection of the main atrial activity (AA) component given by principal component analysis, which is shown to provide detailed information about AA potential pattern distributions on the body surface. Different AA potential pattern distributions can then be identified, depending on the underlying degree of AF organization. An automated way to assess AF organization degree is then proposed, based on topographic projections. Similarities with previous studies suggest its usefulness for determining uniform distributions in the activation patterns on the body surface.**

I. INTRODUCTION

Atrial fibrillation (AF) severity increases with time and so does the consequent impairment of the cardiac function, causing several electro-structural changes in the myocardium which may lead to serious complications. AF progression is the reason why a widely accepted successful treatment strategy for this pathology is still lacking nowadays. Thus, in relation to the duration of its episodes, AF is differently treated [1]. Moreover, inconsistent success rates of different therapies underline that AF treatment is challenging, when it comes to avoiding unnecessary and risky procedures. A proper noninvasive diagnosis would make AF treatment more effective in selecting good candidates for a certain procedure. An appropriate therapy relies on the knowledge of AF characteristics, as its degree of organization, a marker of AF progression. To this purpose, fast and accurate imaging of cardiac electrical activity could be helpful to provide detailed information about the exact electrical functioning of the heart, which is essential for a correct diagnosis.

A detailed information on AF organization can be obtained by intravenous approaches, but such an invasive approach is nowadays considered too drastic for diagnostic purposes. Hence, more recent works have attempted a noninvasive evaluation of AF organization through body surface potential maps (BSPM) [2], which have the advantage over the conventional ECG of a much higher spatial resolution. Guillem *et al.* [3] have demonstrated the possibility of visually evaluating different activation patterns in AF patients. Moreover, we have recently shown that the spatio-temporal organization in the AA during AF can be noninvasively and quantitatively evaluated from BSPM recordings [4]. This has been carried out looking at the reflection on the surface ECG of the spatio-temporal complexity of the recorded atrial activity (AA) in the BSPM recording, by means of principal component analysis (PCA). Complexity is meant as the amount of disorganization observed on the ECG, and is supposed to be directly correlated to the number and interactions of simultaneous atrial wavefronts. However, BSPMs suffer of the smoothing effect of the torso volume conductor which smears the body surface distribution of the potentials, and thus it is still limited by a low spatial resolution to resolve and localize multiple simultaneous active myocardial electrical events.

In this paper, we introduce a way to partially overcome this problem. The spatial topography related to the most important component given by the PCA of the AA in the BSPM recording is retained and its topographic projection on the ensemble of electrodes is obtained. This is justified by the fact that the global perspective on the underlying AA given by surface ECG recordings can be supposed to mainly reflect the behavior of the atrial areas characterized by an AF type similar to the predominant one observed on the body surface. A visual inspection of the obtained maps suggests the presence of differences among the analyzed patients. These differences turn out to be correlated to the level of AF organization of each patient, as previously identified in [4]. Hence, this visual representation allowed us to focus on discriminating among patients in terms of their organization in time and space, unlike in [4] where the discrimination was based on the reconstruction error of the projections of the different AA segments over a reference segment. The topographic projections associated with organized AF seem to show uniform distribution in their maps, while disorganized

P. Bonizzi, R. Westra, and J. Karel are with the Department of Knowledge Engineering, Maastricht University, P.O. Box 616, 6200 MD, Maastricht, The Netherlands. pietro.bonizzi@maastrichtuniversity.nl

O. Meste and V. Zarzoso are with Laboratoire I3S, UNSA/CNRS, 2000 Route des Lucioles, Les Algorithmes Euclide B, B.P. 121, 06903 Sophia Antipolis Cedex, France.

M. S. Guillem and F. Castells is with ITACA - Bioingenieria, Universitat Politecnica de Valencia, 46022 España.

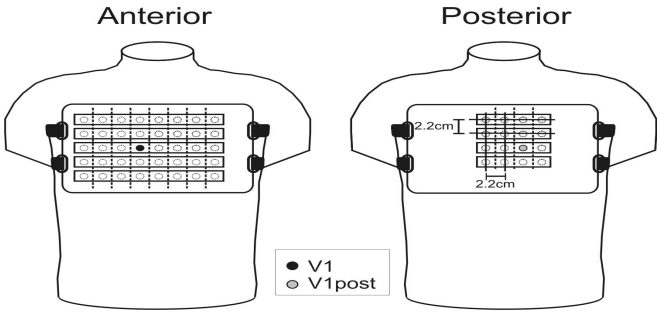

(a)

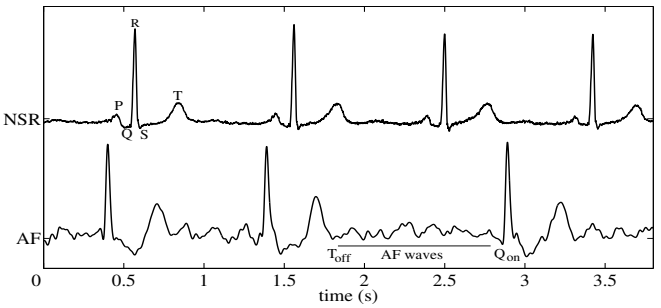

(b)

Fig. 1. (a) Arrangement of the electrodes and belt used for their attachment to the patient. Electrode positions are represented as open circles while V1 and V1post are denoted by black and grey circles, respectively. Electrodes were placed around V1 and V1post as a uniform grid. (b) Definition of the different cardiac waves and intervals of interest. At the top, example of normal sinus rhythm ECG recording (NSR), showing the different cardiac waves. At the bottom, example of ECG recording during AF, showing a TQ interval (off:offset; on:onset).

AF patients do not show any particular trend. Thus, after a suitable transformation, these differences can be exploited to distinguish among organized and disorganized AF. An automated way to achieve this classification is then proposed, which provides comparable results as those obtained in [4].

II. METHODS

A. Data and acquisition system

The same dataset composed of 14 patients as the one introduced in [4] was employed in this study (10 males, 4 females; age 68±14 years; AF duration 12±18 months). One BSPM signal was recorded for each patient. All recordings presented persistent AF. The acquisition system consisted of a total of 56 leads (anterior: 40, posterior: 16) acquired simultaneously for each subject, as shown in Fig. 1(a).

Signals were acquired at a sampling frequency of 2048 Hz and preprocessed by applying a third-order zero-phase band-pass Chebyshev filter with frequency band between $[0.5, 100]$ Hz, to remove baseline wandering and high frequency noise.

B. Atrial activity description through principal component analysis and topographic projections

As in [4], only TQ segments in the BSPM recording were analyzed, where no ventricular activity is present. Each recording was split in 6 consecutive 10s-length intervals, and an AA signal was obtained for each interval concatenating only the TQ segments inside it (see Fig. 1(b) for the definition of the different cardiac waves and intervals). Thus, each lead l in the s^{th} AA recording (with $s = 1, \ldots, 6$) is represented by a row vector:

$$\mathbf{y}_l^{(s)} = [y_l^{(s)}(1), \ldots, y_l^{(s)}(N)] \tag{1}$$

where N is the number of samples inside the interval. Then, the entire ensemble of leads is compactly represented by the $56 \times N$ matrix:

$$\mathbf{Y}^{(s)} = \begin{bmatrix} \mathbf{y}_1^{(s)} \\ \vdots \\ \mathbf{y}_{56}^{(s)} \end{bmatrix}$$

The interested reader is referred to [4] for further details about the procedure to generate $\mathbf{Y}^{(s)}$.

One manner to analyze the information about AA inside matrix $\mathbf{Y}^{(s)}$ is to transform it in a set of components by minimizing the redundancy among them. This can be achieved by PCA. Indeed, spatial uncorrelation provided by PCA involves a linear transformation of the mean corrected observed signals $\mathbf{Y}^{(s)} \in \mathbb{R}^{n \times N}$ ($n = 56$, in this study), which produces a set of mutually uncorrelated waveforms with unit variance $\mathbf{X}^{(s)} \in \mathbb{R}^{m \times N}$ with ($m \leq n$), so that:

$$\mathbf{Y}^{(s)} = \mathbf{M}^{(s)} \mathbf{X}^{(s)} \tag{2}$$

where $\mathbf{X}^{(s)} = \begin{bmatrix} \mathbf{x}_1^{(s)} \\ \vdots \\ \mathbf{x}_m^{(s)} \end{bmatrix}$ is an estimate of the true vector of the unknown components, and $\mathbf{M}^{(s)} = (n \times m)$ is the transfer matrix. In this model, the transfer matrix accounts for both the volume conductor properties and the solid angle under which the single component contributes to the potential on each lead. Thus, the i^{th} column of $\mathbf{M}^{(s)}$ represents the spatial topography (ST) that links the i^{th} component of $\mathbf{X}^{(s)}$ with the observed signals $\mathbf{Y}^{(s)}$. The spatio-temporal stationarity of the AA potential field is to be reflected in the coefficients stored in each ST. Thus, the ST $\mathbf{M}_{1:n,1}^{(s)}$ associated with the first principal component (PC) $\mathbf{x}_1^{(s)}$ is the one best reflecting the main distribution of the AA potential field on the body surface. Its entries provide information about the relative contribution of the first PC to the potential of each electrode, and on which electrodes that PC is mainly reflected. The relative locations of these electrodes may inform us on the presence of uniform distributions of the activation patterns. For this purpose, a topographic projection of the weights stored in the first ST is obtained so as to produce a visual map of the importance of each electrode in observing the first PC. Weights' values are linearly reassigned by a suitable color coding, as defined below, so that the higher the weight stored in the ST the lighter the color associated with the corresponding electrode (the more tends to red). Conversely, the lower the weight the darker the associated color (the more tends to dark blue). Extremely noisy leads have been discarded and appear as white electrodes. The reassignment is carried out as follows. Firstly, a color map matrix $\mathbf{H} = (M \times 3)$

is obtained (e.g., using *colormap* function in MatLab, with default setting JET, and a coding based on $M = 64$ colors), organized so that the first rows describe darkest colors, while the last rows describe lightest colors. Then, for each AA segment, a linear mapping is produced so as to assign each weight in the first topography $\mathbf{M}^{(s)}_{1:n,1}$ to a specific color (a row in matrix $\mathbf{H}$). This is carried out by means of a linear model as

$$\mathbf{l}^{(s)} = a^{(s)}\mathbf{M}^{(s)}_{1:n,1} + b^{(s)} \tag{3}$$

where parameter a is set so that

$$a^{(s)} = \frac{M-1}{\max(\mathbf{M}^{(s)}) - \min(\mathbf{M}^{(s)})} \tag{4}$$

and $b^{(s)}$ derived, e.g., as

$$b^{(s)} = 1 - a^{(s)}\min(\mathbf{M}^{(s)}) \tag{5}$$

Vector $\mathbf{l}^{(s)}$ is thus the vector of reassigned positions (rows) in $\mathbf{H}$. Thus, electrodes are colored so as to be scaled with respect to the value of the corresponding coefficient in the projected ST.

C. Automated analysis of uniform distributions and AA potential pattern organization

After obtaining the topographic projection of $\mathbf{M}^{(s)}_{1:n,1}$, as in the previous section, the corresponding vector $\mathbf{l}^{(s)}$ of reassigned positions was clustered into two bins. This was conducted in MatLab environment exploiting function *histc*, with an optimal step equals 40, which provided the highest similarities with [4]. This analysis was separately carried out for the 40 electrodes in the front and the 16 in the back. Thus, the first bin, corresponding to lower rows in matrix $\mathbf{H}$, describes mainly dark colors, that is, less significant weights in $\mathbf{M}^{(s)}_{1:n,1}$, while the second mainly describes light colors, that is, more significant weights in $\mathbf{M}^{(s)}_{1:n,1}$. Hence, the number of reassigned positions falling in each bin was considered, providing an information on the mean trend of each AA segment (either predominance of dark or light colors, or resemblance). The degree of the AF potential pattern organization was then analyzed in terms of similarities (uniform distributions) in the clustering over the different segments on the same patient. Due to physiological considerations (see Section IV), this analysis was mainly based on back electrodes, while front electrodes were used to solve indeterminacies. Finally, the linear reassignment presented in the previous section is a transformation which allows a normalization of the STs, so as to perform automated analysis of their distributions.

III. RESULTS

A. Visual inspection of the topographic projections

Topographic projections of the first PC of each of the 6 AA segments on the ensemble of electrodes produce visual maps as those shown in Figs. 2(a)-2(c). Investigating the different projections for the 14 patients in the dataset, interesting remarks appear. When focusing on the topographic projections obtained for the electrodes on the back, three different kind of distributions along the 6 segments seem to be present: unimodal, bimodal, multimodal:

1) unimodal: all back electrodes show uniform intensity (almost same color) over a certain segment; this unimodal distribution is kept over all segments for a certain patient. An example is depicted in Fig. 2(a);
2) bimodal: all back electrodes show two main intensities (two different colors) over a certain segment; this bimodal distribution is kept over all segments for a certain patient. An example is depicted in Fig. 2(b);
3) multimodal: absence of any recursive structure of the back electrode intensities over all segments. An example is depicted in Fig. 2(c).

B. Automated analysis of uniform distributions in the topographic projections

As introduced in Section II-C, the number of reassigned positions in each bin over the different segments was exploited to estimate the level of AF organization in a certain patient, as follows: a patient showed a unimodal distribution if over all the segments all the back electrodes were clustered in one bin. Conversely, if the number of elements in each bin was equal, or equal but one, the patient was said to present a bimodal distribution. In both cases the patient was said to present an organized AF. Otherwise, in every other case the patient was said to present a multimodal distribution, and so characterized by a disorganized AF. We obtained strong similarities with the spatio-temporal identification previously found in [4], with 12 out of 14 patients labeled in the same way by both methodologies (6 patients showed organized AF, and 8 patients showed disorganized AF). If information from front leads was also properly included in the analysis, correlation between the two methodologies improved. Indeed, exploiting the reassigned positions on front leads in order to estimate the dispersion of the signal on the chest, 14 out of 14 patients have been labeled in the same way by both methodologies (8 patients showed organized AF, and 6 patients showed disorganized AF). In order to do that, we considered as organized AF patients those who, besides showing a back unimodal distribution, presented all anterior position mainly classified in the same bin over all segments.

IV. DISCUSSION AND CONCLUSIONS

An effective treatment of AF asks for proper noninvasive analysis of the AF temporal progression in terms of AF degree of organization. To this extent, fast and accurate imaging of cardiac electrical activity is demanded. Thanks to their high spatial resolution, BSPM recordings can be exploited to partly solve this problem. This work proposed a method to obtain a spatial representation of the main AA component given by PCA, which after a suitable normalization provided a detailed information about AA potential pattern distributions on the body surface. Particularly, three main structures have been identified. Unimodal and bimodal distributions, which present a relative recursive structure, that can be interpreted as uniform distributions in the main activation patterns on the body surface. Patients showing these kind of

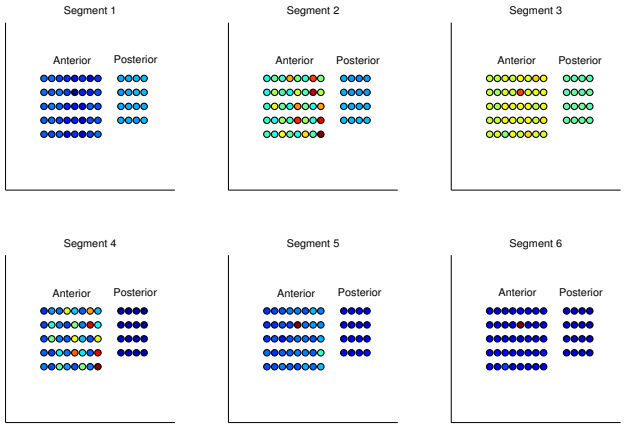

(a)

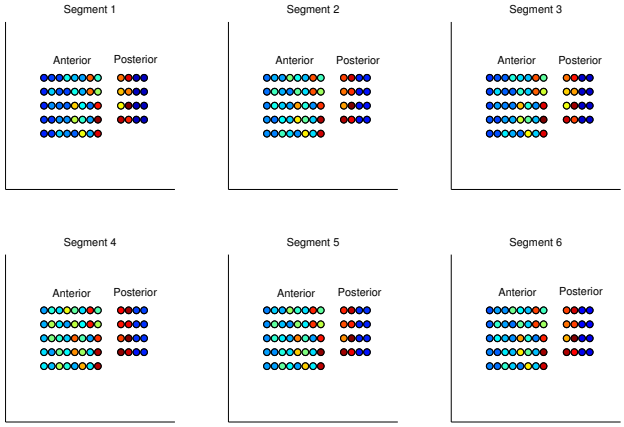

(b)

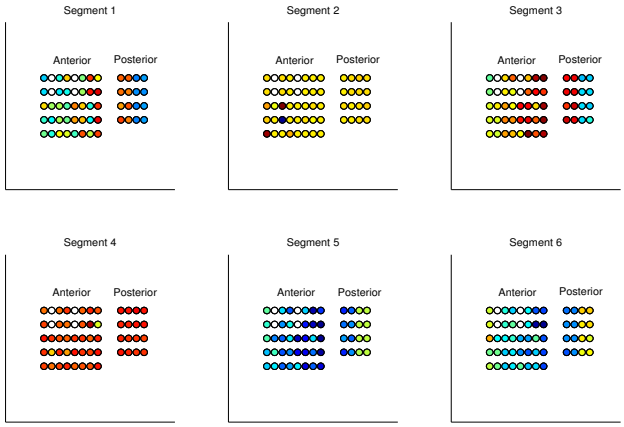

(c)

Fig. 2. Visual projection of the weights stored in the first spatial topography derived from segments 1 to 6, respectively, of patient 2 (a), patient 9 (b), and patient 13 (c), on the associated surface electrodes.

behaviors generally corresponded to those identified in [4] as characterized by an organized AF. Conversely, multimodal distributions do not show any particular recursive structure, underlining a more disorganized distribution in the wavefront propagation inside the atria, as reflected on the body surface. Patients showing this kind of behavior corresponded to those identified in [4] as characterized by a disorganized AF. Moreover, in [4] we exploited the reconstruction error of the projections of the different AA segments over a reference segment to achieve AF organization estimation, focusing on lead V1 only. However, we did not represent data in space, while this representation at the present time allowed us to focus on discriminating among patients in terms of their organization in time and space, by looking at the maps generated by the projection of the first ST. These preliminary results may pave the way for a possible estimation of more detailed information about simultaneous activations (AA vector direction and activation areas' locations), especially for patients showing more organized AF. For instance, patient 9 (Fig. 2(b)), characterized by organized AF, showed a first PC direction which keeps quite constant over time. This underlines a relative stationarity of the main AA potential pattern, which shows a bimodal distribution and seems to be located mainly in the left atrium. This is in line with the pathophysiology of AF, since the pulmonary veins have been revealed to be an important source of spontaneous electrical activity that initiates AF [5]. Their position close to the left atrium makes back leads suitable to observe them, also explaining why back leads reveal to be more significant in an automated analysis of uniform distributions. The automated classification presented in Sec. III-B may be affected by being strongly data driven. Further work is demanded in order to make it more robust, and in this sense a wider dataset is needed, possibly including simultaneous invasive electrograms in order to have an objective reference for a classification of the patients in different AF classes. Finally, these results may be useful to improve AF diagnosis and a priori efficient treatment selection.

REFERENCES

[1] V. Fuster, L. E. Ryden, D. S. Cannom, H. J. Crijns, and A. B. et al. Curtis. ACC/AHA/ESC 2006 guidelines for the management of patients with atrial fibrillation: A report of the American College of Cardiology/American Heart Association Task Force on practice guidelines and the European Society of Cardiology Committee for practice guidelines (writing committee to revise the 2001 guidelines for the management of patients with atrial fibrillation): developed in collaboration with the european heart rhythm association and the heart rhythm society. *Circulation*, 114:e257–e354, 2006.

[2] R. L. Lux. Electrocardiographic body surface potential mapping. *Crit. Rev. Biomed. Eng.*, 8:253–279, 1982.

[3] M. S. Guillem, A. M. Climent, F. Castells, D. Husser, J. Millet, A. Arya, C. Piorkowski, and A. Bollmann. Noninvasive mapping of human atrial fibrillation. *J. Cardiovasc. Electrophysiol.*, 20(5):507–513, 2009.

[4] P. Bonizzi, M. S. Guillem, A. M. Climent, J. Millet, V. Zarzoso, F. Castells, and O. Meste. Noninvasive assessment of the complexity and stationarity of the atrial wavefront patterns during atrial fibrillation. *IEEE Trans. Biomed. Eng.*, 57(9):2147–57, 2010.

[5] M. Haïssaguerre, P. Jaïs, D. C. Shah, S. Garrigue, A. Takahashi, T. Lavergne, M. Hocini, J. T. Peng, R. Roudaut, and J. Clémenty. Electrophysiological end point for catheter ablation of atrial fibrillation initiated from multiple pulmonary venous foci. *Circulation*, 101(12):1409–1417, Mar 2000.